

# Lensing effects in inhomogeneous cosmological models

Sima Ghassemi<sup>1\*</sup>, Salomeh Khoeini Moghaddam<sup>2†</sup>, and Reza Mansouri<sup>1,3‡</sup>

<sup>1</sup>*School of Astronomy and Astrophysics, Institute for Research in Fundamental Sciences (IPM),  
P. O. Box 19395-5531, Tehran, Iran,*

<sup>2</sup>*Physics Dept., Faculty of Science, Tarbiat Moalem University, Tehran, Iran,*

<sup>3</sup>*Department of Physics, Sharif University of Technology,  
Tehran 11365-9161, Iran*

Concepts developed in the gravitational lensing techniques such as shear, convergence, tangential and radial arcs maybe used to see how tenable inhomogeneous models proposed to explain the acceleration of the universe models are. We study the widely discussed LTB cosmological models. It turns out that for the observer sitting at origin of a global LTB solution the shear vanishes as in the FRW models, while the value of convergence is different which may lead to observable cosmological effects. We also consider Swiss-cheese models proposed recently based on LTB with an observer sitting in the FRW part. It turns out that they have different behavior as far as the formation of radial and tangential arcs are concerned.

## I. INTRODUCTION

There is an on-going debate in the community whether inhomogeneities on scales up to several hundred mega parsecs could account, at least partially, for the observed dimming of the SNe Ia [Celerier [1], Sarkar [2]]. Irrespective of successes of these models to explain the dark energy, it is desirable to have some independent cosmological tests of these models. The obvious effect of the inhomogeneities is the light propagation which may differ significantly in a clumpy universe compared with a homogeneous FRW model. Recently Vanderveld et al [3], being interested in the possibility of explaining the supernova data, have studied light propagation in one of the Swiss cheese models recently proposed [4] using weak field gravitational lensing techniques. We are interested in the potential gravitational lensing effects in inhomogeneous models to see if there are crucial effects which could constrain or rule out some of the models.

In this paper we focus on LTB-based inhomogeneous models. The LTB solution of Einstein equations describes an inhomogeneous spherically symmetric dust filled cosmological model with a distinguished center of symmetry. Having a center of symmetry, thus not reflecting the homogeneity of the universe at large, these models are mainly used as toy models to study the local inhomogeneities of the universe. After a short review of LTB inhomogeneous solutions, and Swiss-cheese models based on it, we look at the general question of how different does a LTB model behave relative to a FRW model as far as gravitational lensing concepts are concerned (section III). For an observer at the origin of a flat LTB metric, the shear vanishes as in the case of a FRW metric. However, the convergence is different from that of the FRW due to the  $r$ -dependence of metric coefficients and the corresponding scale factor. The vanishing

of the shear is only true for an observer at the origin of LTB. The more general and interesting case of an off-center observer has to be treated separately. This case, however, maybe treated in Swiss cheese models based on LTB which is the subject of the section IV, where arcs in strong lensing regime are investigated for two different Swiss-cheese models, assuming the observer and the source are sitting in the cheese (FRW metric). While the onion model [5] turns out to produce neither tangential nor radial arc, the model proposed by Marra, Kolb, Matarrese and Riotto [4] do produce both radial and tangential arcs. The models we have considered could be looked at as providing different density profiles of a lens, to be compared with the profiles published so far and mainly based on simulations. The Swiss cheese models, e.g., provide us with density profiles which maybe compared for special parameters to the NFW one which is a phenomenological density profile well supported by the simulations [6].

## II. A REVIEW ON INHOMOGENEOUS LTB MODELS

The LTB metric ( $c = 1$ ) in co-moving and proper time coordinates with zero cosmological constant is given by

$$ds^2 = -dt^2 + S^2(r, t)dr^2 + R^2(r, t)(d\theta^2 + \sin^2\theta d\phi^2). \quad (1)$$

Considering dust stress-energy tensor, Einstein's equations imply the following constraints:

$$S^2(r, t) = \frac{R'^2(r, t)}{1 + 2E(r)}, \quad (2)$$

$$\frac{1}{2}\dot{R}(r, t) - \frac{GM(r)}{R(r, t)} = E(r), \quad (3)$$

$$4\pi\rho(r, t) = \frac{M'(r)}{R'(r, t)R^2(r, t)}, \quad (4)$$

where dot and prime denote partial derivatives with respect to  $t$  and  $r$  respectively. Function  $\rho(r, t)$  is energy density of the matter. Functions  $E(r)$  and  $M(r)$  are left arbitrary.  $M(r)$  can be interpreted as the mass inside of co-moving sphere with coordinate radius  $r$ . Assuming  $M'(r) > 0$ ,  $M(r)$  can be chosen as

$$M(r) = \frac{4\pi}{3}M_0^4 r^3. \quad (5)$$

Now, taking this as the definition of the coordinate radius, we may write solutions of Einstein's equations depending on  $E(r)$  in the following ways:

1. For  $E > 0$  the solution is

$$R = \frac{GM(r)}{2E(r)}(\cosh u - 1) \quad (6)$$

$$t - t_n(r) = \frac{GM(r)}{[2E(r)]^{3/2}}(\sinh u - u); \quad (7)$$

2. For  $E = 0$  we have

$$R(r, t) = \left[\frac{9}{2}GM(r)\right]^{1/3}[t - t_n(r)]^{2/3}; \quad (8)$$

3. Finally for  $E < 0$  the solution is

$$R = \frac{GM(r)}{-2E(r)}(1 - \cos u) \quad (9)$$

$$t - t_n(r) = \frac{GM(r)}{[-2E(r)]^{3/2}}(u - \sin u). \quad (10)$$

The so-called bang time function  $t_n(r)$  is an integration constant, indicating different singularities defined by  $t = t_n$  [7].

As we are going to discuss phenomenon far from these singularities, we may assume  $t \gg t_n$ . Therefore, we will assume from now on  $t_n = 0$ .

### A. Small- $u$ approximation

Relation between the coordinate  $r$  and the parameter  $u$  in the non-flat LTB cases is not trivial. It has been shown that for the special case of  $E(r)$  being a trigonometric function of  $r$ , small  $u$  approximation is even valid for enough large  $r$  [5]. This, however, is not in general the case as may be seen for a polynomial function  $E(r)$ . However, to simplify the calculation, we are going to assume  $u$  to be a small parameter. This approximation, which can describe the dynamics even when  $\delta\rho/\rho \gg 1$ , allows to solve the Einstein's equations [5,8].

Physically  $u^2$  is related to spatial curvature  $E(r)/r^2$  [5,8]. In addition we assume  $E > 0$ , leading to the following equations:

$$R(r, t) = \frac{2\pi r}{3k(r)}(\cosh u - 1), \quad (11)$$

$$\tilde{M}t = \frac{\sqrt{2}\pi}{3k(r)^{3/2}}(\sinh u - u), \quad (12)$$

where

$$k(r) := \frac{E(r)}{\tilde{M}^2 r^2}, \quad (13)$$

$$\tilde{M} := \frac{M_0^2}{m_{pl}}, \quad (m_{pl} = \sqrt{\frac{1}{G}}). \quad (14)$$

Keeping next to leading terms in  $u$ , we obtain from (11) and (12)

$$R \approx \frac{\pi r}{3k(r)}u^2 \left(1 + \frac{u^2}{12}\right),$$

$$\tau^3 := \tilde{M}t \approx \frac{\pi\sqrt{2}}{18k(r)^{3/2}}u^3.$$

As mentioned before, the relation between parameter  $u$  and spatial curvature  $k(r)$  is given by

$$u = \frac{18}{\pi\sqrt{2}}\tau\sqrt{k(r)}.$$

Therefore, the small  $u$  approximation is valid when

$$u = \gamma\tau\sqrt{k(r)} \ll 1, \quad (15)$$

where

$$R_2 := \frac{1}{12} = 0.08, \quad \gamma := \left(\frac{9\sqrt{2}}{\pi}\right)^{1/3} \approx 1.59.$$

Substituting  $u$  yields,

$$R(r, t) = \frac{\pi}{3}\gamma^2\tau^2 r[1 + R_2\gamma^2\tau^2 k(r)]. \quad (16)$$

### B. Swiss-cheese model

The inhomogeneous metrics may be used to model universe in different ways. The direct way is to take an inhomogeneous metric, say a LTB solution of Einstein equation, as the model universe and see the effect of lensing in it. One may, however, devise a so-called Swiss-cheese model in which the bulk (cheese) is represented by a matter-dominated flat homogeneous FRW model and the spherically symmetric holes are constructed using a specific LTB solution. The holes which represent the inhomogeneities are distributed randomly in the bulk, so the model is isotropic and homogenous on average. The matching of the inhomogeneous holes to the FRW bulk must be handled with care [9]. Depending on different types of LTB solutions, one may construct different

Swiss-cheese models.

Biswas et. al [8] study a Swiss-cheese model in which the holes are represented by a LTB metric in the small  $u$  approximation regime (section II A). They choose  $M_0$  in such a way that the coordinate density,  $M_0^A$ , coincides with the average density ( $\rho_0$ ) at present time  $t_0$ :

$$M_0^A = \rho_0 = \frac{M_p^2}{6\pi t_0^2}, \quad (17)$$

or

$$\tau_0^2 = t_0 \tilde{M} = \frac{1}{\sqrt{6\pi}}.$$

The matching conditions imply [10]

$$k'(L) = 0,$$

where  $L$  is the comoving radius of the hole and prime means derivative with respect to  $r$ . Using the above normalization (17) for  $\Omega_k \ll 1$  ( $\Omega_k$  is curvature abundance of the homogeneous universe at the same time) we arrive at

$$k(L) = \frac{4\pi}{3}\Omega_k.$$

In order to be consistent with CMB we choose

$$k(L) = 0.$$

According to [10], continuity at the origin implies another constraint on curvature:

$$k'(0) = 0$$

Recently Marra et.al [4] defined a different Swiss-cheese model in which arbitrary number of spherical holes with different size and density profile are distributed in the cheese. The cheese evolves as FRW while the holes evolve differently. At the boundary of the holes, as a consequence of the boundary conditions, the average mass density, defined by  $\bar{\rho} = \frac{3}{R(r,t)^3} \int_0^r \rho(r,t) R^2 R' dr$ , coincides to the FRW density, and  $E(r)$  has to go to zero. As far as local physics is concerned, the hole has no effect on the observer outside it.

### III. LTB UNIVERSE - OBSERVER AT THE ORIGIN

Let us first study the lensing effect due to the global inhomogeneity in a flat LTB solution ( $E(r) = 0$ ):

$$ds^2 = dt^2 - R'(t,r)^2 dr^2 - R(t,r)^2 d\Omega^2. \quad (18)$$

We do not assume any single or multiple lens but are interested in the global effect of bending of light rays due

to the LTB inhomogeneities. For simplicity, we place the observer at the event  $O$  (center of the inhomogeneous region) with 4-velocity  $u_o^\alpha$ ,  $u_o^\alpha u_{\alpha o} = 1$ . Choosing the affine parameter of the rays,  $\lambda$ , at  $O$  such that (1)  $\lambda = 0$  at origin, (2)  $\lambda$  increases to the past and (3)  $k_\alpha u_o^\alpha|_O = -1$ , then  $k^\alpha = \frac{dx^\alpha}{d\lambda}$  is past directed. Using the dimensionless  $k^\alpha$ , the corresponding wave vector is then defined by  $-\frac{\omega_o}{c} k^\alpha$ , where  $\omega_o$  is the frequency of the wave measured by the observer at  $O$ .

Let  $\gamma_0$  be a ray and  $u^\alpha$  on  $\gamma_0$  be the result of the parallel propagated four velocity of the observer,  $u_o^\alpha$ . The orthonormal bases along  $\gamma_0$  on the lens plane are  $E_1^\alpha$  and  $E_2^\alpha$ . The deviation vectors of the beam centered on  $\gamma_0$  can then be written as  $Y^\alpha = -\xi_1 E_1^\alpha - \xi_2 E_2^\alpha - \xi_0 k^\alpha$ , where  $\xi_1$  and  $\xi_2$  are called the screen components of the corresponding separation vector of two neighboring light rays [11]. For the above metric these vectors are derived as

$$E_1^\alpha = \left[ 0, 0, \frac{1}{\sqrt{g_{\theta\theta}(z)}}, 0 \right], \quad E_2^\alpha = \left[ 0, 0, 0, \frac{1}{\sqrt{g_{\phi\phi}(z)}} \right], \quad (19)$$

and

$$k^\alpha = (1+z) \left[ -1, \frac{1}{\sqrt{g_{rr}(z)}}, 0, 0 \right], \quad (20)$$

where  $z$  is the red-shift of the source ( $O$ ) defined as:

$$(1+z) = \frac{(k_\alpha u^\alpha)_e}{(k_\alpha u^\alpha)_o}. \quad (21)$$

The evolution of  $\xi = (\xi_1, \xi_2)$  is given by the following equation of geodesic deviation [12]:

$$\ddot{\xi}(\lambda) = \mathcal{T}(\lambda)\xi(\lambda), \quad (22)$$

where  $\mathcal{T}$  is the optical tidal matrix describing the influence of space-time curvature on the propagation of light:

$$\mathcal{T}(\lambda) = \begin{pmatrix} \mathcal{R}(\lambda) + Re\mathcal{F}(\lambda) & Im\mathcal{F}(\lambda) \\ Im\mathcal{F}(\lambda) & \mathcal{R}(\lambda) - Re\mathcal{F}(\lambda) \end{pmatrix}. \quad (23)$$

$\mathcal{R}$  is the so-called source of convergence:

$$\mathcal{R} = -\frac{1}{2}R_{\mu\nu}k^\mu k^\nu, \quad (24)$$

where  $R_{\mu\nu}$  is the Ricci tensor of the metric.  $\mathcal{F}$  is the source of shear:

$$\mathcal{F} = -\frac{1}{2}C_{\alpha\beta\gamma\delta}\epsilon^{*\alpha}k^\beta\epsilon^{*\gamma}k^\delta, \quad (25)$$

where  $\epsilon^\alpha := E_1^\alpha + iE_2^\alpha$  and  $C_{\alpha\beta\gamma\delta}$  is the Weyl curvature tensor of the metric. As expected, for isotropic metrics, like LTB with the observer at the origin, the source of shear is vanishing:

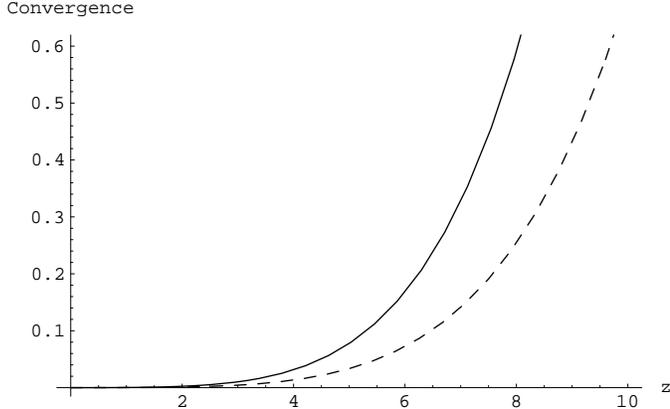


FIG. 1. Source of convergence as a function of red-shift. The solid curve stands for the FRW model and the dashed curve for flat LTB.

$$\mathcal{F}_{LTB} = 0. \quad (26)$$

In the case of flat LTB spacetime with corresponding solutions (8) the relevant source of convergence is, however, non-vanishing:

$$\mathcal{R} = (1+z)^2 \left[ \frac{\ddot{R}}{R} - \frac{\dot{R}\dot{R}'}{RR'} \right]. \quad (27)$$

The non-vanishing convergence means that the light coming from a source at  $(r, t)$  is converged by (27) when observed at the origin  $O$ . To derive the relevant red-shift  $(z)$  for each event  $(t$  and  $r)$  we used the numerical code of ([7]). We have then plotted the convergence as a function of increasing  $z$  (Fig.1). As it is shown in the picture, convergence is increasing with  $z$ . This convergence is different from that of the FRW spacetime. To understand this difference one needs to study different observables such as time delay of images of a source, which goes beyond the scope of this paper, and we will go into its detail in a future publication.

#### IV. SWISS-CHEESE MODEL OF THE UNIVERSE: OBSERVER IN THE CHEESE

In the previous section we studied a special problem where the observer was at the center of inhomogeneities. To be more realistic we want to study a more general problem where the observer is placed somewhere between inhomogeneities in the universe and observes a distant source. The light coming from the source is passing the inhomogeneous regions in between and reaches the observer. For simplicity, we consider two different Swiss-cheese models (section II B)) in which the observer and the source are in the cheese and the light passes through one of the holes: Onion model of Biswas et al. [8] who derive a perturbative LTB solution of Einstein equations

and study the evolution of the density contrast within the holes, and the model of Marra et al. [4] who construct a non-perturbative solution in the holes. In this model the universe is completely filled with these holes which form a sort of lattice, taking care of the matching conditions between LTB and FRW metrics on the boundary of the hole. The hole is almost empty except at the boundary where the matter is concentrated and has an average density matching that of FRW density.

We will trace light rays within these two Swiss cheese models coming from a source in the Homogenous Friedman background, the cheese, passing a lens, a hole, and finally detected by an observer in the cheese. Deriving the source of convergence and shear in this case, is not a simple job due to the difficulty of tracing light rays in the Swiss cheese which is not as straightforward as in the case of the LTB model with the observer at the origin. For arbitrary observer we expect a non-vanishing shear. The effect of the shear is best studied through observables such as radial and tangential arcs [13] of the distant galaxies. We will first elaborate on some of the basic definitions and then go on to calculate the arcs in models just described.

#### A. Some basic definitions in lensing

The surface mass density of the lens is defined as

$$\Sigma(\xi) = \int_{-\infty}^{+\infty} \rho(r, t) dz, \quad (28)$$

where  $r = \sqrt{z^2 + \xi^2}$ ,  $z$  is the coordinate aligned with the line of sight and  $\xi$  are the coordinates in the lens plane (with the origin on the lens). Convergence of the light bundles made by the lens is defined as follows:

$$\kappa(\xi) = \frac{\Sigma(\xi)}{\Sigma_{critical}} \quad (29)$$

where  $\Sigma_{critical}$  is defined as:  $\Sigma_{critical} := \frac{c^2}{4\pi G} \frac{D_s}{D_d D_{ds}}$  [13]. Now consider that we are observing a far galaxy and the light coming from that galaxy to us is bent due to the lensing of the inhomogeneity which exists in their path. There are some places in the lens plane where the magnification of the lens goes to infinity. Then what we see in the lens plane are some radial or tangential arcs. The magnification of a lens is defined as follows [13]:

$$\mu \propto \frac{1}{\det(\mathcal{A})}, \quad (30)$$

where  $\mathcal{A}$  is the Jacobian of the transformation of the source plane coordinates to the lens plane ones. When the determinants of  $\mathcal{A}$  goes to zero we will have the arcs in the lens plane (called critical curves). Therefore, to derive possible arcs, one should calculate the eigenvalues

of  $\mathcal{A}$  first and see if it can be zero somewhere on the lens plane or not.

The mass inside radius  $x$  is described by the dimensionless function:

$$m(x) := 2 \int_0^x \kappa(\xi) d\xi. \quad (31)$$

It can be easily shown that the eigenvalues of the  $\mathcal{A}$  matrix be derived using this dimensionless function [13,6]:

$$\lambda_r = 1 - \frac{d}{dx} \frac{m(x)}{x}, \quad \lambda_t = 1 - \frac{m(x)}{x^2}. \quad (32)$$

$\lambda_r$  and  $\lambda_t$  are called radial and tangential critical curves, respectively. When  $\lambda_r$  goes to zero the arcs of an extended source in the lens plane are radial and when  $\lambda_t$  goes to zero the arcs of an extended source in the lens plane are tangential.

### B. Radial and tangential arcs I: Onion Swiss cheese model

To study the arcs, we trace light rays coming from a far source (in the Homogenous Friedman background - the cheese) passing a lens with perturbative LTB metric, as described in section (II A), and finally detected by an observer in the cheese. Once we have the density profile of such a lens, we can immediately derive the place of arcs and see if there exists both radial and tangential arcs or not [6]. Different density profiles have been studied before. For example the NFW profile [14] can produce radial and tangential arcs [6].

Density profile of a LTB lens with perturbative metric (section (II A)) is given by the following relation, derived from the Einstein equations in the small  $u$  approximation:

$$\rho(r, t) = \frac{M_0^4}{\pi G (\tilde{M}t)^2 \left[ 1 + R_2 \gamma^2 (\tilde{M}t)^{2/3} A(r) \right]}, \quad (33)$$

where  $A(r) := \left( \frac{E(r)}{r \tilde{M}^2} \right)'$ .

It seems that the density is decreasing with time, while we expect the structure grows as a function of time. But the important point here is that the relevant quantity to study the structure growth is the density contrast.

The background spacetime is a FRW spacetime. Hence, one can define the density contrast as the deviation of the holes density ( $\rho(r, t)$ ) from the cheese density ( $\langle \rho \rangle (t)$ , averaged over the holes) [5]:

$$\delta := \frac{\rho(r, t) - \langle \rho \rangle (t)}{\langle \rho \rangle (t)}, \quad (34)$$

defining  $\epsilon(r, t) := R_2 \gamma^2 (\tilde{M}t)^{2/3} A(r)$ , one can derive the density contrast:

$$\delta = \frac{-\epsilon(r, t)}{1 + \epsilon(r, t)}. \quad (35)$$

As Biswas et al. show [5],  $A(r)$  has to be bounded to get underdensity (voids) and overdensity (structure) regions:

$$A_{min} < A(r) < A_{max} \rightarrow \delta_{min} < \delta < \delta_{max} \quad (36)$$

As  $\epsilon(r, t)$  is an increasing function of time, its sign is crucial to get the underdensity and overdensity regions. A negative  $\epsilon(r, t)$  gives a positive density contrast which grows with time (growing structures) and a positive  $\epsilon(r, t)$  gives a negative density contrast growing with time (growing voids). Therefore,  $A_{min}$  should be negative, corresponding to an overdense region.

As it is shown in [5], the following  $E(r)$  can satisfy the above condition (36):

$$E(r) = \tilde{M}^2 \frac{A_1 L}{2\pi} r \sin^2 \left( \frac{\pi r}{L} \right), \quad (37)$$

where  $L$  is a typical length of the large scale structures and  $A_1$  is the amplitude of the density oscillations. This may be seen by looking at  $R(r, t)$ :

$$R(r, t) \approx (6\pi)^{1/3} (\tilde{M}t)^{2/3} r \left[ 1 + \frac{A(t)}{2\pi} \frac{L}{r} \sin^2 \left( \frac{\pi r}{L} \right) \right], \quad (38)$$

where  $A(t) := R_2 \gamma^2 A_1 (\tilde{M}t)^{2/3}$ . The density profile can also be written as

$$\rho(r, t) = \frac{M_0^4}{6\pi (\tilde{M}t)^2 \left[ 1 + A(t) \sin^2 \left( \frac{2\pi r}{L} \right) \right]}, \quad (39)$$

showing the significance of  $A(t)$  as the amplitude of oscillations.

The special characteristic of this Swiss cheese model is that each hole has an onion like density profile which at the large  $r$ 's goes to a homogeneous background density.

Now, consider one of these LTB regions as a lens. The plane perpendicular to the line of sight of the source (which can be a far galaxy) is called the lens plane. The light passes through the FRW region and, close to the lens, it is bent due to the density profile of the LTB hole using the small  $u$  approximation, just as in the Schwarzschild case.

In realistic cases one may forget about the time evolution of the lens during the passage of light. This means the characteristic time of lens evolution is much greater than the light passage time. In the following we will apply this approximation.

We have now all the quantities to calculate  $\lambda_r$  and  $\lambda_t$  for the density profile (39). Figures 3-6 show the behavior of  $m(x)$ ,  $\lambda_r$ , and  $\lambda_t$  as a function of the distance to the center of the lens in the lens plane,  $x$ .

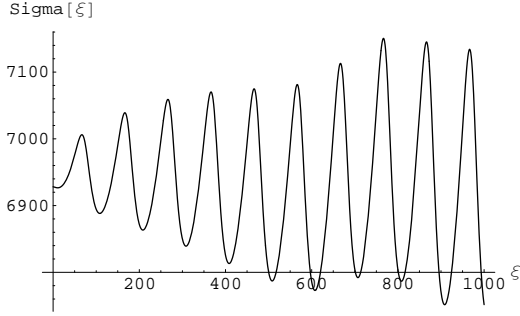


FIG. 2. Surface mass density of the lens as a function of the coordinates on the lens plane.

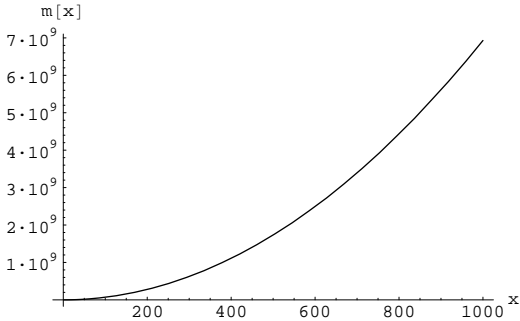


FIG. 3. Mass of the lens inside radius  $x$  in the sinusoidal Swiss-cheese model.

As expected,  $m(x)$  increases as a function of  $x$ . Obviously there is no solution to the equations  $\lambda_r = 0$  and  $\lambda_t = 0$ , as can be seen from the Fig 4 and Fig 5.  $\lambda_r = 0$  may have a solution in the large 'x' which is by far out of the range of our approximation.

The result of no arcs, neither radial nor tangential, means that the onion Swiss cheese model with sinusoidal solution is ruled out by observations.

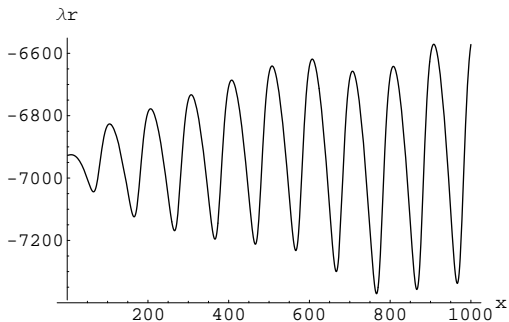


FIG. 4. Behavior of  $\lambda_r(x)$  with respect to  $x$  in the Swiss-cheese model.

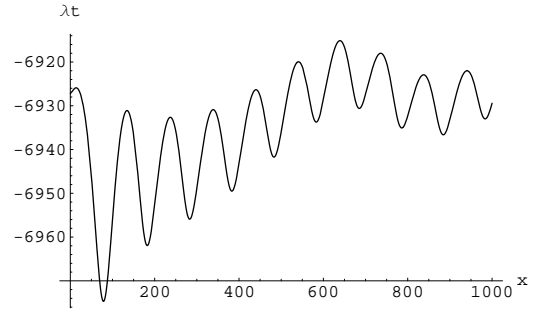


FIG. 5. Behavior of  $\lambda_t(x)$  with respect to  $x$  in the Swiss-cheese model.

### C. Radial and tangential arcs II: Swiss cheese model of Marra et al

We assume again that the time of light passage through the hole is negligible relative to time evolution of the density of the hole in the model of MKMR [4]. To derive the solution of Einstein equations within the holes obeying the junction conditions, they choose the initial density function to have a gaussian profile:

$$\begin{aligned} \rho(r, t_i) &= A \exp[-(r - r_M)^2 / 2\sigma^2] + \epsilon \quad (r < r_h) \\ \rho(r, t_i) &= \rho_{FRW}(t_i) \quad (r > r_h), \end{aligned} \quad (40)$$

where  $\epsilon = 0.0025$ ,  $r_h = 0.42$ ,  $\sigma = r_h/10$ ,  $r_M = .037$ ,  $A = 50.59$ , and  $\rho_{FRW}(t_i) = 25$ . The hole ends at  $r_h = .042$  which is equivalent to  $350 \text{ Mpc}$ . This is not a big hole but is almost an empty region: the matter density in the hole is  $10^4$  times smaller than in the cheese.

Applying this initial condition to the Einstein equations (in the curved LTB case:  $E(r) \neq 0$ ), one gets  $v(r, t)$  (the peculiar velocity),  $R(r, t)$ , and  $\rho(r, t)$ . Hence, we have the density profile of the lens at  $t = 0$  which, in their notation, is the present time (Fig 6).

We have done the calculation along the same line as in the last section, assuming the source and the observer far from the hole and in the FRW background (cheese). As can be seen from the Figs 7 and 8, this model allows both radial and tangential arcs. However, this happens at  $r > r_h$  which means that the arcs will be observed out of the inhomogeneous region.

## V. CONCLUSION AND DISCUSSION

Independent of how successful the inhomogeneous models are in explaining the dark energy problem, gravitational lensing may serve as a criterion to distinguish inhomogeneous cosmological models. Different concepts developed in the cosmological gravitational lensing techniques such as shear, convergence, tangential and radial arcs, and time delays maybe used to see how tenable

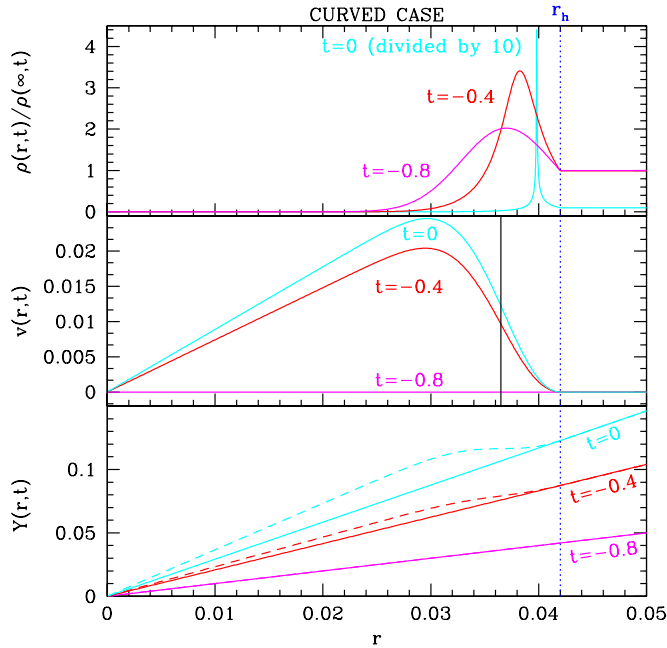


FIG. 6. Behavior of  $R(r,t)$  ( $Y(r,t)$ ) in MKMR model, peculiar velocity  $v(r,t)$  and the density profile  $\rho(r,t)$  with respect to  $r$  for the curved case at  $t_i = -0.8$  and  $t = 0$  (present time). The straight lines in the  $R(r,t)$  diagram are FRW solutions [4].

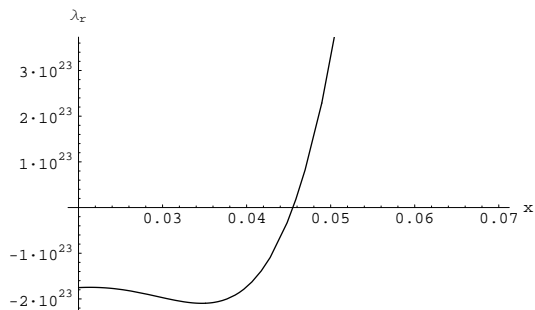


FIG. 7. Behavior of  $\lambda_r(x)$  with respect to  $x$  in Marra et al model.

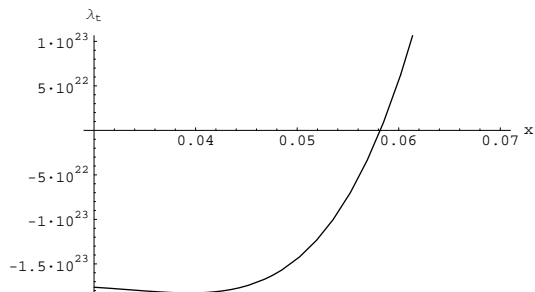


FIG. 8. Behavior of  $\lambda_t(x)$  with respect to  $x$  in Marra et al model.

these models are. The widely discussed LTB cosmological models, having a vanishing shear as the FRW models, differ from FRW ones in the value of convergence which may lead to observable effects such as different time delays of the cosmological images and the large scale lensing effects in the CMB. Assuming the observer outside the center of symmetry of LTB, one expect a universal shear not seen in the FRW models.

The Swiss cheese models provide us with a density profile for a "hole", to be compared with the NFW profile. Therefore, the question of tangential and radial arcs may lead us to a test of such models, or to a better fixing of the model parameters. The onion model predicts neither a tangential nor a radial arc. We may therefore rule it out even as a toy model to explain dark energy. The MKMR Swiss-cheese model [4] do produce both radial and tangential arcs. The arcs are located in the cheese outside the hole near the massive shell. The size of the hole is about 350 Mpc, much bigger than familiar structures in the universe. Therefore, it is not possible to compare this result with real data. It may be possible, however, to fix the parameter of the model such that more realistic arcs results. If these parameters are compatible with the explanation of the dimming of the supernovas is another question. We therefore conclude that it is desirable to do more research on different aspects of gravitational lensing effects in inhomogeneous models of the universe.

## ACKNOWLEDGEMENT

SK-M thanks IPM astronomy school for hospitality. RM would like to thank Iran TWAS chapter and ISMO for financial support.

- 
- [1] M. Celerier, *New Advances in Physics* **1**, 29 (2007), astro-ph/0702416 .
  - [2] S. Sarkar, *Gen. Rel. Grav.* **40** (2008) 269-284, arXiv:0710.5307.
  - [3] R. A. Vanderveld, E. E. Flanagan and I. Wasserman, *Phys.Rev.* **D78** (2008) 083511. arXiv:0808.1080.
  - [4] V. Marra, E. Kolb, S. Matarrese, A. Riotto, *Phys.Rev.* **D76** (2007) 123004, arXiv:0708.3622.
  - [5] T. Biswas, R. Mansouri and A. Notari, *JCAP* **12** (2007) 017, astro-ph/0606703.
  - [6] M. Bartelmann, *Astron. Astrophys.* **313** (1996) 697, astro-ph/9602053.
  - [7] Khosravi, Kourkchi, Mansouri, Akrami, *Gen. Rev. Grav* **40** (2008), astro-ph/0702282
  - [8] T. Biswas and A. Notari, *JCAP* **06** (2008) 021, astro-ph/0702555.

- [9] S. Khakshournia and R. Mansouri, *Phys.Rev.* **D65** (2002) 027302, gr-qc/0307023.
- [10] R. A. Vanderveld, E. E. Flanagan and I. Wasserman , *Phys.Rev.***D74** 023506 (2006), asro-ph/0602476.
- [11] Seitz, Schneider and Ehlers, *Class.Quant.Grav.***11** (1994) 2345-2374, astro-ph/9403056.
- [12] P. Schneider, J. Ehlers and E. E. Falco, Gravitational Lenses, Springer, 1st Edition 1992, 2nd Printing 1999.
- [13] M. Bartelmann, P. Schneider, *Phys.Rept.* **340** (2001) 291-472 ,astro-ph/9912508.
- [14] J. Navarro, C. S. Frenk, S.D.M. White, *MNRAS* **275** (1995), 720, astro-ph/9408069.